Sensitivity analysis of turbulence using unstable periodic orbits: a demonstration on the Kuramoto-Sivashinsky equation

Davide Lasagna

Aerodynamics and Flight Mechanics Research Group
Faculty of Engineering and Environment - University of Southampton
University Road, Southampton, SO17 1BJ, United Kingdom
davide.lasagna@soton.ac.uk

ABSTRACT

A robust approach for adjoint-based sensitivity analysis of chaotic dynamics based on unstable periodic orbits is proposed. We show that a careful reformulation of established variational techniques to such trajectories enables the sensitivity of time averages with respect to design parameters to be calculated exactly, *regardless of the stability characteristics and length of the orbit*. This holds the promise of bringing recent advances in the study of the dynamics and role of exact solutions of the Navier-Stokes equations to bear in design and optimisation problems for turbulent flows.

In this paper, we derive the adjoint technique and discuss, as a proof of concept, a feedback control design problem for the Kuramoto-Sivashinsky equation, i.e. a prototypical one-dimensional partial differential equation with rich dynamical behaviour. Key challenges and opportunities associated to the application of this method to fluid turbulence, left as future work, are also discussed.

INTRODUCTION

Significant advances in understanding transitional and fully-developed turbulent shear flows at moderate Reynolds numbers have been obtained in the last fifteen years by tackling the problem from a dynamical systems perspective (Kawahara *et al.*, 2011). Research in this area has been initiated by the numerical discovery of three-dimensional, nonlinear, steady (Nagata, 1990) and time-periodic (Kawahara & Kida, 2001) unstable solutions of the equations in plane Couette flow. The interest is primarily driven by the fact that these solutions often reproduce the dynamics and the recurrent coherent structure observed in turbulent flows, which justifies names under which they are collectively referred to, i.e., *exact coherent structures* (Waleffe, 2001), or *recurrent flows* (Chandler & Kerswell, 2013). The established picture is that these flows form the constitutive elements of a robust skeleton, a web that organises and supports the temporal evolution of turbulence (Willis *et al.*, 2013). These flows have thus become in recent years a prominent basis to analyse, describe and understand turbulence. The promise, rooted in the machinery offered by Periodic Orbit Theory (Auerbach *et al.*, 1987), is that a handful of these flows is "enough" to obtain a complete picture of a turbulent flow (Cvitanović, 2013).

However, a question that remains open in the community is whether and how these flows will prove fruitful for purposes such as design and control. In this paper, we offer a possible answer to such a question and propose to use a particular class of such flows, i.e. unstable periodic orbits (UPOs), as a basis for **parametric sensitivity analysis** of turbulence. Sensitivity analysis provides the gradient of output quantities of interest, e.g. the mean turbulent skin-friction drag, with respect to the design parameters of the problem, e.g. the geometry of the surface bounded by the flow. It provides fundamental insight into complex dynamical behaviour and enables gradient-based optimisation, control and design.

The key enabler is that a careful application of adjoint techniques to a time periodic trajectory enables the gradient of the period average to be calculated exactly, *regardless of the stability characteristics and length of the orbit*. In stark contrast, application of adjoint techniques to unstable open trajectories fails to provide the correct gradient (Lea *et al.*, 2000). The fundamental reason is that in the latter case the adjoint problem is an *initial value problem* marched backwards in time from an homogeneous terminal condition and the adjoint solution grows unbounded exponentially in time, due to the positive Lyapunov exponents of the system, resulting in wrong gradients. By contrast, for a periodic orbit the adjoint problem is a *two-point boundary value problem* and admits time periodic solutions that remains bounded regardless of the instability.

It is worth noting that there is a clear distinction between our aims and that of previous chaos control studies, where the idea is to stabilise by feedback a particular unstable orbit with desirable period-averaged properties (e.g. Shinbrot *et al.* (1993)). Here, we aim to exploit UPOs to understand how the "turbulent attractor" and its statistics change at first order when the parameters of the problems are varied. In theory, strange attractors with dissipative dynamics posses an infinity of UPOs and appropriate weighted sums can be introduced to express ergodic statistics of the system (Auerbach *et al.*, 1987). In this paper, we leave such consideration of more fundamental nature apart and focus exclusively on the development and analysis of the adjoint sensitivity technique.

Problem settings are first presented. The adjoint problem for an UPO is then derived and appropriate numerical techniques for its solution are discussed. The method is then demonstrated on a model problem relevant to applications, i.e. the design of a feedback controller for the Kuramoto-Sivashinsky equation (KSEq). The KSEq is a prototypical one dimensional partial differential equation exhibiting chaotic behaviour and arising in a variety of physically relevant contexts, e.g., reaction-diffusion systems (Kuramoto, 1978) and the dynamics of liquid films falling along a wall (Sivashinsky & Michelson, 1980). It is considered here primarily because the modest size of the discretisation makes it a convenient playground to test ideas and develop algorithms before delving into more challenging three dimensional turbulence problems, left as future work. Specifically, UPOs of the KSEq are used to extract the sensitivity of an observable of the system with respect to the gains of a controller driving in-domain actuation. Statistics over the UPOs found are analysed, and key features arising from the problem symmetries are elucidated. Finally, the sensitivity information is used to construct a controller that mitigates the dynamics. The concluding section discusses key challenges and implications for turbulent flows.

PRELIMINARIES

For convenience, the methodology is outlined here in finite dimensional settings, i.e. the system is assumed to be described by a set of ordinary differential equations (ODEs). Formally the same methodology applies to partial differential equations (PDEs), e.g. the Navier-Stokes and continuity equations for an incompressible

flow. Let thus the system be defined as

$$\mathbf{x}_{\mathrm{dt}}(t) = \mathbf{f}(\mathbf{x}(t);\mathbf{p}) \tag{1}$$

where $\mathbf{x}(t)$ is the state vector in the state space $\mathbb{R}^{N_\mathbf{x}}$, t is time and subscript $(\cdot)_{\mathrm{d}\cdot}$ denote total differentiation. The subscript $(\cdot)_{\partial\cdot}$ will denote in what follows partial differentiation. The vector field $\mathbf{f}:\mathbb{R}^{N_\mathbf{x}}\times\mathbb{R}^{N_\mathbf{p}}\to\mathbb{R}^{N_\mathbf{x}}$ is a smooth vector function of $\mathbf{x}$ and depends additionally on a vector $\mathbf{p}\in\mathbb{R}^{N_\mathbf{p}}$, the design/control parameters, or variables, of the problem. These variables parametrise the system, its dynamics and its "performance" measured by some observable $K(t)=K(\mathbf{x}(t)):\mathbb{R}^{N_\mathbf{x}}\to\mathbb{R}$. For a turbulent flow problem, the design variables might represent the geometry, boundary conditions, feedback control parameters, surface roughness features, properties of a compliant material, etc. and the observable could be, for instance, the spatially averaged instantaneous skin friction drag.

For turbulent systems, it is typical to consider the time average of the instantaneous cost

$$\overline{K} = \frac{1}{T}\int_0^T K(\mathbf{x}(t))\mathrm{d}t \tag{2}$$

over some chaotic trajectory $\mathbf{x}(t)$, with a sufficiently large horizons T to reach adequate convergence. The sensitivity $\overline{K}_{\mathrm{d}\mathbf{p}}$, i.e. the gradient of the time average with respect to the parameters $\mathbf{p}$, is the quantity of interest that enables optimisation and can provide physical insight on the system dynamics. As discussed in the introduction, for chaotic systems it is not possible to obtain such a gradient using standard adjoint techniques.

The main idea of this paper is to replace the average over a chaotic trajectory with the average over a periodic one. A periodic orbit $\mathbf{x}^o(t)$ of period T is a trajectory of (1) such that $\mathbf{x}^o(t+T)=\mathbf{x}^o(t)$, $\forall t$, for the minimum T. The superscript $(\cdot)^o$ denotes a quantity on a periodic trajectory. For convenience, the Linstedt-Poincaré transformation $s=2\pi t/T=\omega t$, with ω being the frequency of the orbit, is introduced to transform time $t\in[0,T]$ into the loop parameter $s\in[0,2\pi]$, where the origin $s=0$ is arbitrary. This transformation makes the initially unknown period become explicit in the evolution equation on the orbit, i.e,

$$\omega\mathbf{x}^o_{\mathrm{d}s}(s) = \mathbf{f}(\mathbf{x}^o(s);\mathbf{p}), \tag{3}$$

and simplifies the differentiation of integrals pertaining to period averages, denoted by bracket as

$$\langle K\rangle = \frac{1}{2\pi}\int_0^{2\pi} K(\mathbf{x}^o(s))\,\mathrm{d}s, \tag{4}$$

whose upper bound will not depend explicitly on the period T. The key enabler is that an adjoint sensitivity method that is well-behaved can be formulated over such trajectories, to calculate exactly the gradient of the period average $\langle K\rangle_{\mathrm{d}\mathbf{p}}$, regardless of the stability and length of the orbit.

ADJOINT SENSITIVITY FOR UPOs

Previous works on adjoint sensitivity techniques for *stable* periodic orbits include Giannetti *et al.* (2010) for sensitivity and control of vortex shedding past a circular cylinder and Hwang (2014) for sensitivity and control of nonlinear global modes of the Ginzburg-Landau equation. Here, we follow similar formalisms and then discuss appropriate numerical methods for *unstable* orbits.

Assuming a periodic orbit is available, the Lagrangian

$$\mathscr{L}(\mathbf{p}) = \langle K^o + \boldsymbol{\lambda}'\cdot(\omega\mathbf{x}^o_{\mathrm{d}s} - \mathbf{f}^o)\rangle \tag{5}$$

is constructed using the governing equation on the orbit (3) and the adjoint variables $\boldsymbol{\lambda}(s)\in\mathbb{R}^{N_\mathbf{x}}$. In (5), the prime denotes vector transposition, $(\cdot)$ is the standard inner product between vectors, and the notation K^o is a shorthand for $K(\mathbf{x}^o(s))$ (and similarly for other instances). Integrating by parts with respect to time the term $\boldsymbol{\lambda}'\cdot\mathbf{x}^o_{\mathrm{d}s}$ leads to

$$\mathscr{L}(\mathbf{p}) = \left\langle K^o - \omega\boldsymbol{\lambda}'_{\mathrm{d}s}\cdot\mathbf{x}^o - \boldsymbol{\lambda}'\cdot\mathbf{f}^o\right\rangle + \boldsymbol{\lambda}'\cdot\mathbf{x}^o\big|_0^{2\pi}, \tag{6}$$

where the boundary term is key and will be used in what follows to derive appropriate temporal boundary conditions for the adjoint equation. The Lagrangian is then differentiated with respect to the parameters, to obtain the gradient $\langle K\rangle_{\mathrm{d}\mathbf{p}}=\mathscr{L}_{\mathrm{d}\mathbf{p}}$, where we follow the notation that gradients are row vectors. Gathering terms multiplying the state sensitivity $\mathbf{x}^o_{\partial\mathbf{p}}(s)\in\mathbb{R}^{N_\mathbf{x}\times N_\mathbf{p}}$ yields

$$\mathscr{L}_{\mathrm{d}\mathbf{p}} = \Big\langle \overbrace{(K^o_{\partial\mathbf{x}} - \omega\boldsymbol{\lambda}'_{\mathrm{d}s} - \boldsymbol{\lambda}'\cdot\mathbf{f}^o_{\partial\mathbf{x}})}^{=0}\cdot\mathbf{x}^o_{\partial\mathbf{p}} - \boldsymbol{\lambda}'\cdot\mathbf{f}^o_{\partial\mathbf{p}} - (\boldsymbol{\lambda}'\cdot\mathbf{x}^o_{\mathrm{d}s})\boldsymbol{\omega}_{\mathrm{d}\mathbf{p}}\Big\rangle + \underbrace{+\boldsymbol{\lambda}'\cdot\mathbf{x}^o_{\partial\mathbf{p}}\big|_0^{2\pi}}_{=0} \tag{7}$$

where the Jacobian matrices $\mathbf{f}^o_{\partial\mathbf{x}}$ and $\mathbf{f}^o_{\partial\mathbf{p}}$ have size $\mathbb{R}^{N_\mathbf{x}\times N_\mathbf{x}}$ and $\mathbb{R}^{N_\mathbf{x}\times N_\mathbf{p}}$, respectively. The state sensitivity obeys a linear differential equation obtained by differentiating the governing equation (3) with respect to the parameters (Wilkins *et al.*, 2009). It expresses, at first order, the effects of parameters perturbations on the "shape and location" of the UPO in phase space. In the formulation of the sensitivity equations it is implicitly assumed that the perturbed orbit remains periodic and that the orbit does not bifurcate. It can be an expensive quantity to compute (and thus preferred to adjoint techniques), as the cost grows linearly with the number of parameters. The gradient of the frequency with respect to the parameters $\boldsymbol{\omega}_{\mathrm{d}\mathbf{p}}$ appearing in (7) is not not known a priori. In principle, it can be obtained as part of the solution of the sensitivity equations, but can be also obtained more economically as discussed later.

The adjoint variables are then selected such that the two terms indicated by braces in (7) vanish identically, circumventing the expensive calculation of $\mathbf{x}^o_{\partial\mathbf{p}}(s)$. This results in the adjoint problem

$$\boxed{\begin{cases} \omega\boldsymbol{\lambda}_{\mathrm{d}s}(s) = -\mathbf{f}^{o\prime}_{\partial\mathbf{x}}(s)\cdot\boldsymbol{\lambda}(s) + \mathbf{K}^{o\prime}_{\partial\mathbf{x}}(s) & \text{(8a)}\\ \boldsymbol{\lambda}(0) = \boldsymbol{\lambda}(2\pi) & \text{(8b)}\\ 0 = \boldsymbol{\lambda}'(0)\cdot\mathbf{f}^o(0) & \text{(8c)}\end{cases}}$$

where the constraint (8c) breaks the translational invariance of the orbit[1]. The key observation is that periodic boundary conditions (8b) are enforced in the adjoint problem. These arise from requiring

$$0 = \boldsymbol{\lambda}'\cdot\mathbf{x}_{\partial\mathbf{p}}\big|_0^{2\pi} = \boldsymbol{\lambda}'(2\pi)\cdot\mathbf{x}_{\partial\mathbf{p}}(2\pi) - \boldsymbol{\lambda}'(0)\cdot\mathbf{x}_{\partial\mathbf{p}}(0) = [\boldsymbol{\lambda}(2\pi)-\boldsymbol{\lambda}(0)]'\cdot\mathbf{c} \tag{9}$$

[1] Without this condition, problem (8) has a one-parameter family of solutions: if $\boldsymbol{\lambda}(s)$ is a solution, $\boldsymbol{\lambda}(s+\Delta)$ is a solution too, for any $\Delta\in\mathbb{R}$. The phase locking constraint selects one of such solutions and eliminates the degeneracy arising at discretisation.

in (7) and noting that the state sensitivity is 2π-periodic for an UPO, $\mathbf{x}_{\partial\mathbf{p}}(0) = \mathbf{x}_{\partial\mathbf{p}}(2\pi) = \mathbf{c}$ for some unknown $\mathbf{c}$, because it is assumed that under a perturbation of the parameters the orbit moves globally in phase space but remains periodic. In stark contrast, in classical approaches where the adjoint method is used to optimize the controls over a future horizon, e.g. Bewley *et al.* (2001), the initial condition is assumed not to change with the parameters, hence $\mathbf{x}_{\partial\mathbf{p}}(0)$ and an homogeneous terminal condition $\boldsymbol{\lambda}(t_f) = 0$ is assumed at some final time t_f to make an analogous expression of (9) vanish.

The adoption of periodic boundary conditions has two consequences. Firstly the adjoint solution is time periodic, hence it will remain bounded at all times, *regardless of the stability and length of the orbit*. The exponential growth observed on chaotic systems using the adjoint approach on an open trajectory (Lea *et al.*, 2000) is prevented, enabling the correct sensitivity to be calculated. Secondly, to enforce such boundary conditions an ad-hoc approach for the numerical solution is required. Methods that have been traditionally used to solve two point boundary value problems have to be used. For low dimensional systems, Fourier-Galerkin or finite-difference approaches are computationally feasible and lead to structured matrix problems whose solution provides directly the entire adjoint trajectory. The latter is the approach we have used for the Kuramoto-Sivashinky problem. For PDEs, with a large number of degrees of freedom, shooting techniques can be used, leveraging matrix-free techniques to solve the large linear systems that arise by imposing periodicity.

To obtain the still unknown gradient $\omega_{\mathrm{d}\mathbf{p}}$, Fredholm's alternative is used (Hale (1969), pg. 146). Fredholm's alternative expresses a compatibility constraint for the solution of the sensitivity equations. For these equations to have time periodic solutions, the condition $\left\langle \mathbf{y}'(s)\cdot\left[\mathbf{f}^o_{\partial\mathbf{p}}(s) - \omega_{\mathrm{d}\mathbf{p}}\mathbf{x}^o_{\partial s}(s)\right]\right\rangle = 0$ must hold for all 2π-periodic solutions $\mathbf{y}(s)\in\mathbb{R}^{N_\mathbf{x}}$ of the homogeneous adjoint equation $\omega\mathbf{y}_{\mathrm{d}s}(s) = -\mathbf{f}^o_{\partial\mathbf{x}}(s)\cdot\mathbf{y}(s)$. One solution of this equation can be obtained by using a numerical method analogous to that used for (8), with the third constraint replaced by $\mathbf{y}'(0)\cdot\mathbf{f}^{o\prime}(0) = 1$. The gradient of the frequency is then $\omega_{\mathrm{d}\mathbf{p}} = \langle\mathbf{y}'(s)\cdot\mathbf{f}^o_{\partial\mathbf{p}}(s)\rangle / \langle\mathbf{y}'(s)\cdot\mathbf{x}^o_{\partial s}(s)\rangle$.

When the adjoint solution and the gradient of the frequency have been calculated, the gradient of the period average can be then computed as $\langle K\rangle_{\mathrm{d}\mathbf{p}} = \mathscr{L}_{\mathrm{d}\mathbf{p}} = \left\langle -\lambda'\cdot\mathbf{f}^o_{\partial\mathbf{p}} - (\lambda'\cdot\mathbf{x}^o_{\mathrm{d}s})\omega_{\mathrm{d}\mathbf{p}}\right\rangle$.

DEMONSTRATION ON THE KS EQUATION

The adjoint method is now demonstrated in a sensitivity/design problem for the Kuramoto-Sivashinsky equation (KSEq). The particular form of the KSEq considered here is

$$v_{\partial t}(x,t) = (v^2)_{\partial x}(x,t) - v_{\partial^2 x}(x,t) - \kappa v_{\partial^4 x}(x,t) + h(x,t) \qquad (10)$$

where $v(x,t)$ is the scalar field variable, $x\in[0,2\pi]$ denotes space and t is time. The right hand side is composed of a nonlinear convective term, a second order reaction term and a fourth order diffusion term. The term h is a distributed actuation that is used to control the system. The energy density $K(v(x,t)) = (4\pi)^{-1}\int_0^{2\pi} v(x,t)^2\,\mathrm{d}x$ is selected as the observable of the system we wish to target for control. The equation is parametrised by the diffusivity κ. Here, we investigate a "weakly turbulent" regime at $\kappa = (2\pi/39)^2$.

We consider 2π-periodic odd solutions, satisfying $v(-x) = -v(x)$, $v(x+2\pi) = v(x)$, $\forall x$, similar to, for instance, Christiansen *et al.* (1997). Considering odd solutions reduces the continuous translational symmetry $\tau_\Delta : v(x,t)\to v(x+\Delta,t)$, $\Delta\in\mathbb{R}$ to a discrete shift symmetry $S : v(x,t)\to v(x+n\pi,t)$, $n\in\mathbb{Z}$. From a practical point of view, this reduction eliminates relative periodic orbits - a slightly different adjoint formulation that includes the relative speed would be necessary and is left to future investigations.

A short spatio-temporal sequence of the solution, starting from small random perturbations of the unstable equilibrium $v(x,\cdot) = 0$, is shown in figure 1.

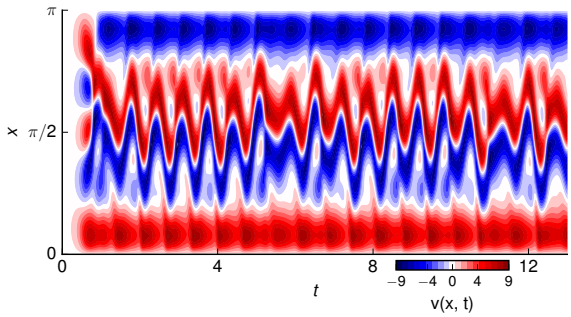

Figure 1. Chaotic realisation of the KSEq at $\kappa = (2\pi/39)^2$.

A feedback controller is introduced to drive actuation as

$$h(x,t) = \mathscr{G}(v(x,t)), \qquad (11)$$

where we assume that $\mathscr{G}$ is linear in $v(x,t)$. The linearity of the feedback does not imply that we seek to find a particular $\mathscr{G}$ that locally stabilises a particular unstable equilibrium or an UPO with desirable period averaged characteristics (Shinbrot *et al.*, 1993). Rather, the aim is to calculate the sensitivity of period averages of the energy density K with respect to the feedback $\mathscr{G}$, i.e. the gradient $\langle K\rangle_{\mathrm{d}\mathscr{G}}$. Loosely speaking, the idea is that analysis of the gradient, in particular over a large set of UPOs, can reveal key control mechanisms that would be otherwise impossible to obtain. The geometric interpretation of this gradient is that, for a given UPO, varying the controller $\mathscr{G}$ in the direction $-\varepsilon\langle K\rangle_{\mathrm{d}\mathscr{G}}$, for some small finite ε has the effect of "moving and reshaping" the UPO in phase space in a way that is optimal for the reduction of $\langle K\rangle$, at least for small ε and excluding structural bifurcations. If most orbits display the same sensitivity, i.e., the same control mechanisms are extracted, varying the controller in the direction of the average gradient results in an overall favourable "displacement" of the attractor. The controlled dynamics will still be chaotic and turbulent but would be mitigated by the actuation, resulting in a reduction of the averaged cost.

A Fourier-Galerkin technique is used for spatial discretisation, i.e. the solution is represented by the expansion $v(x,t) = \sum_{k=-N}^{N} i w_k(t) e^{ikx}$, where $N = 32$, $i = \sqrt{-1}$, k is the integer wave number and the conjugate symmetry $w_{-k} = -w_k$ applies as $v(x,t)$ is real. Note that imposing odd solutions to (10) results in the Fourier expansion coefficients being purely imaginary, hence $w_k\in\mathbb{R}$ and $w_0 = 0$. Application of the Galerkin procedure results in the set of ODEs

$$(w_k)_{\mathrm{d}t} = (k^2 - \kappa k^4)w_k - k\sum_{m=-N}^{N} w_m w_{k-m} + h_k, \quad k = 1,\ldots,N, \qquad (12)$$

where the coefficients h_k arise from a discretisation of the actuation similar to that of the field variable. Spatial discretisation makes the linear functional form of $\mathscr{G}$ explicit, i.e.

$$h_k = \sum_{m=1}^{N} G_{km} w_m, \quad k = 1,\ldots,N, \qquad (13)$$

where the entries of the matrix $\mathbf{G} \in \mathbb{R}^{N_\mathbf{x} \times N_\mathbf{x}}$, the control gains, are now the variables of the problem parametrising (12). Sensitivity results will be thus reported in matrix form with the gradient $\langle K \rangle_{\mathrm{d}\mathbf{G}}$.

Finally, the finite-dimensional equivalent of the discrete shift-by-π symmetry for the PDE is the map

$$S : w_{2m} \to w_{2m}, w_{2m+1} \to -w_{2m+1}, \quad m \in \mathbb{Z} \tag{14}$$

that flips the sign of Fourier coefficients with odd wave number.

Results

A database of $N_o \approx 20000$ unique periodic orbits has been generated using the search algorithm described in Lan & Cvitanović (2004). An integer topological length n is associated to each orbit by counting the number of 'up' intersections with the Poincaré section $w_1 = 0, w_{1\mathrm{d}s}(s) > 0$. Figure 2 shows the search results. On the left axis, the number of UPOs found as function of n is shown. An exponential fit for orbits with $4 \leq n \leq 8$ provides an estimate of the topological entropy (Auerbach *et al.*, 1987) equal to 1.23. The fact that the data follows closely the exponential fit, at least up to $n = 8$, suggests that the vast majority of UPOs of topological length in this range has been found. This provides confidence in the statistics on the available UPOs. On the right axis of the plot, the expectation

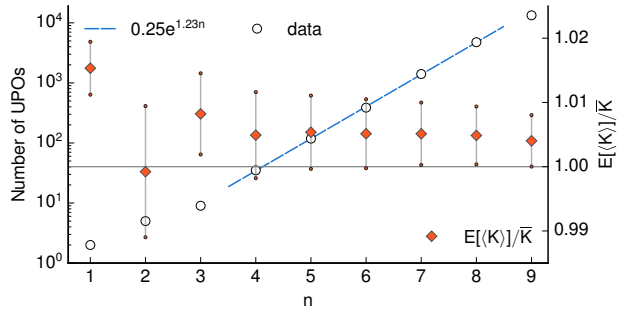

Figure 2. Left axis, open circles (○): number of orbits found as a function of the length n, and exponential fit. Right axis, closed diamonds (◆): expectation of the period average of the energy density, as a function of n, normalised by the long-time average $\overline{K}$.

$\mathrm{E}[\langle K \rangle] = 1/N_o \sum_{i=1}^{N_o} \langle K \rangle^i$ of the period average of the energy density is reported as a function of n, normalised by the long-time average $\overline{K}$ obtained from simulation. The vertical bars show the span of the standard deviation among period averages, for each n. Even short UPOs give remarkably accurate predictions of the average energy density. Longer orbits yield more accurate predictions and the scatter amongst orbits decreases with n. The average spatial structure of long chaotic realisations is also well explained by UPOs, as shown in figure 3-(a), where the time averaged solution $v(x,t)$ for a long chaotic realisation ($T = 1000$) is compared to the period averaged solutions for short ($n = 1$, dashed blue lines) and a random subset of longer ($n = 9$, solid pink lines) orbits. The instantaneous spatio-temporal features of chaotic solutions displayed in figure 1, e.g. the two "boundary layers" at the domain boundaries and the more intense chaotic activity in the domain centre, are also well explained by UPOs, e.g. in 3-(b).

Role of symmetries

The adjoint problem is solved for all UPOs to obtain the gradients $\langle K \rangle_{\mathrm{d}\mathbf{G}}$. We show a few examples and discuss the role that the

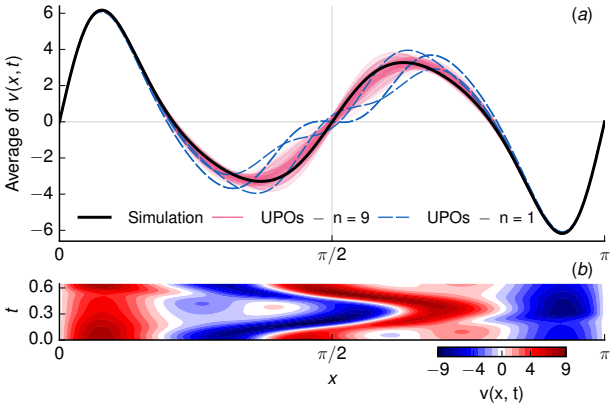

Figure 3. Panel (a): time and period averages of $v(x,t)$ over a long chaotic realisation and selected UPOs of varying length. Panel (b): spatio-temporal dynamics of the shortest UPO, the minimal "building block" of the dynamics, with period $T \approx 0.64$.

symmetries possessed by the equations have on the sensitivity.

Figure 4 shows results for the two shortest UPOs ($n = 1$). The bottom panels show projections on the (w_3, w_4) subspace, whereas the top panels display the entries of gradient $\langle K \rangle_{\mathrm{d}\mathbf{G}}$. The entries of the gradient matrix decay exponentially with m,k, hence only the relevant part is shown. The left panels show the result for an UPO (the same reported in figure 3-(b)) invariant under the symmetry (14). The right panels shows results for an UPO (solid blue line) that does not possess this invariance. The dashed red orbit in the same panel is the symmetric counterpart, obtained by application of (14). Note that only one of the two is counted in the database of UPOs.

For the symmetric orbit the gradient with respect to gains where $k + m$ is odd, indicated by black dots, is identically zero. The non-symmetric orbit does not have this property and all entries

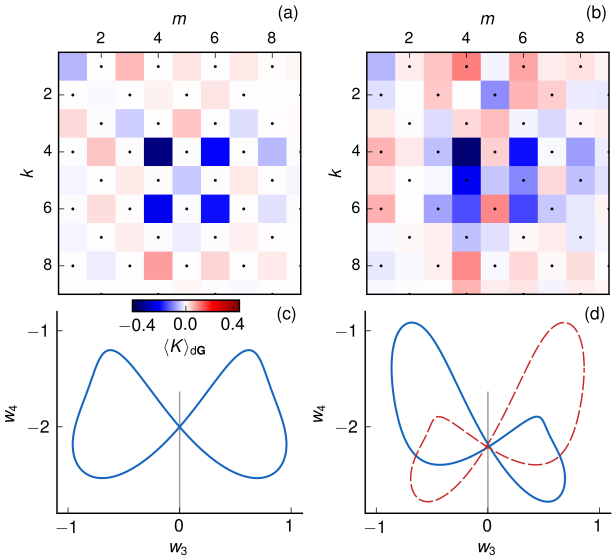

Figure 4. Panels (a)-(b): sensitivity of the period average $\langle K \rangle_{\mathrm{d}\mathbf{G}}$ for the two shortest UPOs ($n = 1$). Panels (c)-(d): projections on the (w_3, w_4) subspace.

are generally non zero. However, the sum of this gradient with that obtained from its symmetric counterpart displays the same pattern.

The origin of this pattern is explained in figure (5), using the symmetric orbit of figure 4-(c). In panel (a), we show the original orbit (thick line), and the two orbits obtained from continuation by perturbing the parameter G_{44} ($G_{44} = +2/-2$, solid red/dashed blue lines, respectively), for which the sensitivity is non-zero. When this parameter is varied, the UPO moves globally in state space towards/away from the origin for positive/negative variations, the period average changes (panel (c)), but the symmetry (14) is preserved (this can be shown from the equations). On the other hand, any small perturbation in G_{43}, panel (b), breaks such symmetry. Depending on the sign of the perturbation the symmetry can be broken in one direction or the other. Now, because the energy density is symmetry-invariant (after discretisation it is defined as $K(t) = \sum_{i=1}^{N} w_k^2(t)$), the period average of the perturbed orbit will not depend on the sign of the perturbation. This implies that the sensitivity must vanish at the origin and second order information becomes important (panel (d)). Our result is similar in nature to recent sensitivity analysis studies of *steady laminar flows*. For instance, Hwang *et al.* (2013) show that at first order the sensitivity with respect to symmetry-breaking perturbations is identically zero.

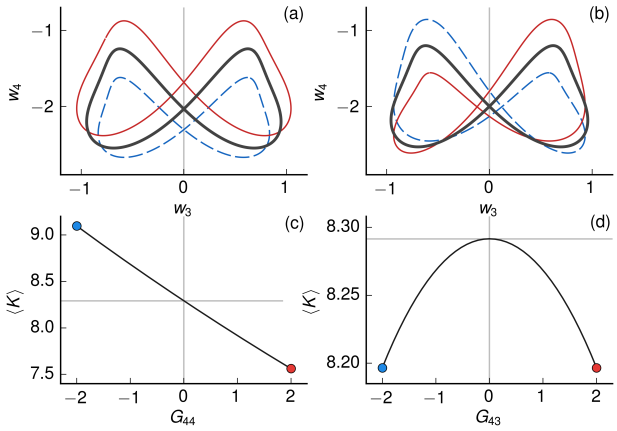

Figure 5. Panels (a-b): projections of the original (thick black line) and perturbed UPOs, for $G_{44} = \pm 2$ and $G_{43} = \pm 2$, respectively. Negative perturbations correspond to the dashed orbits. Panels (c-d): period average of cost as a function of the perturbed parameter. Circles denote the value of the parameter at which projections are shown in the top panels.

This result has significant implications for sensitivity analysis and optimisation of turbulent flows using, but not limited to, the methods discussed here. The primary reason is that in many flow configurations of practical interest, e.g. plane shear flows with homogeneous spatial directions, exact solutions and more importantly the mean flow itself typically possess many of the possible symmetries. Hence, a first order sensitivity analysis might not be sufficient and a second order analysis might be necessary for optimisation over finite amplitude perturbations.

Statistics of gradients and control

The availability of a large number of UPOs enables statistics of the sensitivity to be calculated. Figure 6-(a) shows the expectation of the sensitivity. The same checker board pattern observed for individual orbits is observed. In panels (b) and (c), histograms of two

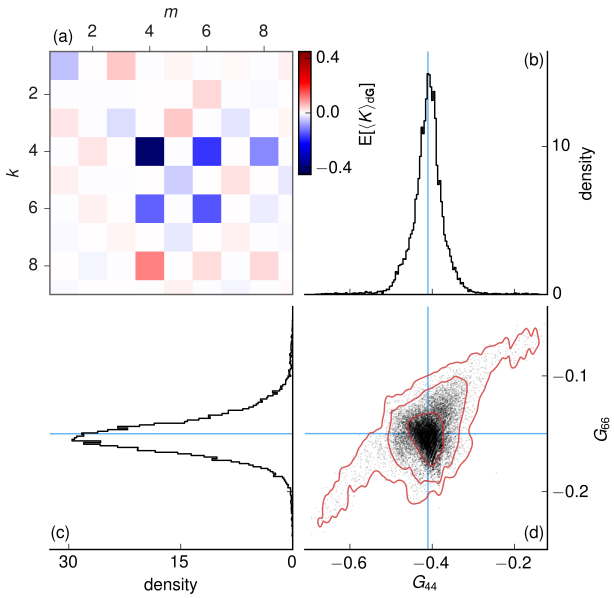

Figure 6. Panel (a): arithmetic average of gradients; Panel (d): projections of the 20000 gradients onto the (G_{44}, G_{66}) subspace (black dots). In red, iso-contours of the joint probability density function of the two components. The contours are for joint density 1, the outer one, 10, and 100, the inner one. Panels (b-c): histograms of the components of the gradient along G_{44} and G_{66}, respectively.

example components, G_{44} and G_{66}, are reported. Panel (d) shows the scatter of these two components and the joint probability density function obtained using a kernel density estimate technique with bandwidth 0.005. The three contours denote density equal to 1, 10 and 100. Analysis of these distributions shows that the vast majority of UPOs predicts approximately the same sensitivity, i.e. the gradients are quite tightly aligned around the expectation of panel (a), denoted by blue lines in the other panels. The average of the gradients might thus be physically relevant and meaningful for feedback control of the chaotic dynamics as a whole.

Hence, using this direction, we construct a controller $\mathbf{G}$ defined as $\mathbf{G} = -\varepsilon \mathrm{E}[\langle K \rangle_{\mathbf{dG}}]$, where ε defines the strength of the control. In other words, we vary the parameters in the direction where on average the UPOs are the most sensitive to, with the idea of "displacing/reshaping" the attractor to mitigate the chaotic dynamics. For small ε, the variation of the period average of the i-th orbit is the projection of the corresponding gradient onto the expectation $\Delta\langle K \rangle^i = \mathrm{vec}(\langle K \rangle^i_{\mathbf{dG}})^T \cdot \mathrm{vec}(-\varepsilon \mathrm{E}[\langle K \rangle_{\mathbf{dG}}])$, where $\mathrm{vec}(\cdot)$ constructs a vector from the columns of a matrix. Its expectation, the average reduction of the period average across UPOs, is thus

$$\mathrm{E}[\Delta\langle K \rangle] = -\varepsilon \| \mathrm{E}[\langle K \rangle_{\mathbf{dG}}] \|^2, \tag{15}$$

where the squared norm $\| \cdot \|^2$ of a matrix is the sum of the squares of its entries. This quantity is now compared with the reduction of the time averaged energy density obtained from long (T=500) numerical simulations of the controlled PDE, as a function of ε. The results are reported in figure 7, where the vertical axis has been normalised by the long-time average of the uncontrolled system. The dashed line is the slope associated to the UPO sensitivity in equation (15).

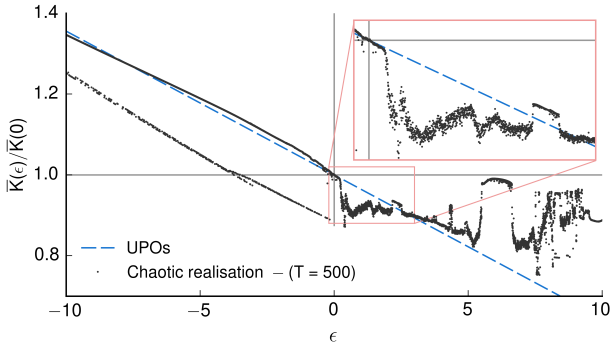

Figure 7. Variation of the normalised long-time average as a function of ε, the strength of the control, from numerical simulation of the controlled PDE (black dots). The dashed line is the average reduction associated to the UPOs

Firstly, the slope associated to the expectation of the gradients gives a good overall representation of the linear variation of the long-term dynamics of chaotic solutions induced by the feedback control, over a surprisingly large range of ε, especially for negative values. This suggests that the spatio-temporal features that the sensitivity analysis has determined to be key for control, remain important and prominent in the solution even in highly controlled conditions.

Secondly, the variation of the strength of the control induces repeated structural bifurcations, with the time average $\overline{K}$ varying non smoothly with ε. This phenomenon is particularly evident for $\varepsilon > 0$. Analysis of the spatio-temporal features of the solution, not reported here for the sake of brevity, reveals that the dynamics can change abruptly, even for small variations of ε. This is an example of structural instability, whereby small structural changes of the equations can induce large variations of the global character of its solutions. This can happen at well defined points for simple dynamics, e.g. the bifurcation from a steady to a time-periodic flow. However, for chaotic dynamical systems, one should in general not expect statistics to be smooth functions of the parameters (Kuznetsov, 2012).

CONCLUSIONS

In this paper we have discussed a well-behaved adjoint technique for sensitivity analysis of chaotic systems. The main idea is to use unstable periodic orbits of the system as a basis to extract sensitivity information. The enabler is mainly that the periodicity of the underlying trajectory entails that the adjoint problem has periodic solutions. Fundamentally, this eliminates the need of a backward-in-time integration and requires the use of appropriate numerical techniques to enforce the periodicity. The key consequence, though, is that the adjoint solution remains bounded regardless of the stability characteristics of the orbit. As a result, the instability of the adjoint solution typically observed on open chaotic trajectories is prevented, enabling the correct sensitivity to be obtained.

This approach awaits application to a turbulent flow problem. There are however several remarks to be made, many of which apply at a general level to all investigations on exact solutions of the equations. For instance, periodic orbits need to be obtained in the first place, which is an expensive task. It is also increasingly difficult to obtain such orbits at increasing Reynolds number and it is still an open question whether such orbit exists, and what they mean, in large extended domains. Furthermore, many periodic orbits exist and it is thus questionable what the sensitivity information extracted from the few that are available means, especially in situations where dynamics are highly intermittent and complex. A statistical analysis like the one provided here can indeed be helpful but very expensive to obtain for a 3D turbulent flow. We wish to address these and other practical issues in future work.

REFERENCES

Auerbach, D, Cvitanović, P, Eckmann, J P, Gunaratne, G & Procaccia, I 1987 Exploring chaotic motion through periodic orbits. *Physical Review Letters* **58** (23), 2387–2389.

Bewley, T R, Moin, P & Temam, R 2001 DNS-based predictive control of turbulence: an optimal benchmark for feedback algorithms. *Journal of Fluid Mechanics* **447**, 179–225.

Chandler, G J & Kerswell, R R 2013 Invariant recurrent solutions embedded in a turbulent two-dimensional Kolmogorov flow. *Journal of Fluid Mechanics* **722**, 554–595.

Christiansen, F, Cvitanović, P & Putkaradze, V 1997 Spatiotemporal chaos in terms of unstable recurrent patterns. *Nonlinearity* **10** (1), 55–70.

Cvitanović, P 2013 Recurrent flows: the clockwork behind turbulence. *Journal of Fluid Mechanics* **726**, 1–4.

Giannetti, F, Camarri, S & Luchini, P 2010 Structural sensitivity of the secondary instability in the wake of a circular cylinder. *Journal of Fluid Mechanics* **651**, 319–337.

Hale, J K 1969 *Ordinary Differential Equations*. Wiley-Interscience.

Hwang, Y 2014 Structural sensitivities of soft and steep nonlinear global modes in spatially developing media. *European Journal of Mechanics B/Fluids* **49**, 322–334.

Hwang, Y, Kim, J & Choi, H 2013 Stabilization of absolute instability in spanwise wavy two-dimensional wakes. *Journal of Fluid Mechanics* **727**, 346–378.

Kawahara, G. & Kida, S. 2001 Periodic motion embedded in plane Couette turbulence: regeneration cycle and burst. *Journal of Fluid Mechanics* **449**, 291–300.

Kawahara, G, Uhlmann, M & van Veen, L 2011 The significance of simple invariant solutions in turbulent flows. *Annual Review of Fluid Mechanics* **44**, 203–225.

Kuramoto, Y 1978 Diffusion-induced chaos in reaction systems. *Progress of Theoretical Physics Supplement* .

Kuznetsov, S P 2012 *Hyperbolic Chaos*. Berlin, Heidelberg: Springer Science & Business Media.

Lan, Y. & Cvitanović, P. 2004 Variational method for finding periodic orbits in a general flow. *Physical Review E* **69** (1), 016217–10.

Lea, D J, Allen, M R & Haine, T W N 2000 Sensitivity analysis of the climate of a chaotic system. *Tellus Series a-Dynamic Meteorology and Oceanography* **52** (5), 523–532.

Nagata, M 1990 Three-dimensional finite-amplitude solutions in plane couette flow: Bifurcation from infinity. *Journal of Fluid Mechanics* **217**, 519–527.

Shinbrot, T, Grebogi, C, Ott, E & Yorke, J A 1993 Using small perturbations to control chaos. *Nature* **363** (6428), 411–417.

Sivashinsky, G I & Michelson, D M 1980 On Irregular Wavy Flow of a Liquid Film Down a Vertical Plane. *Progress of theoretical physics* **63** (6), 2112–2114.

Waleffe, F 2001 Exact coherent structures in channel flow. *Journal of Fluid Mechanics* **435**, 93–102.

Wilkins, A K, Tidor, B, White, J & Barton, P I 2009 Sensitivity Analysis for Oscillating Dynamical Systems. *SIAM Journal on Scientific Computing* **31** (4), 2706–2732.

Willis, A P, Cvitanović, P & Avila, M 2013 Revealing the state space of turbulent pipe flow by symmetry reduction. *Journal of Fluid Mechanics* **721**, 514–540.